ChemistrySelect

Research Article
doi.org/10.1002/slct.202204869

Chemistry Europe
European Chemical Societies Publishing

www.chemistryselect.org

Graphene Quantum Dots Derived from Honey and Mangostin as Sustainable Materials to Construct Fluorescence Turn-On Molecular Switches for Pesticide Detection

Chandranpillai Lalithabai Lekshmi, Unnikrishnapillai Saraswathy Swathy, Keerthi Vijayan, Haleema Simimole, and Sarojiniamma Sumalekshmy*[a]

Extensive use of pesticides in agriculture can lead to environmental pollution and potentially adverse health effects. A fluorescence Turn-On molecular switch, derived from naturally occurring α-mangostin (**MN**), isolated from the pericarp of mangosteen fruit and Graphene Quantum Dots (**GQDs**) synthesized from honey, was developed for the detection of carbofuran-an organic toxic carbamate pesticide. **GQD**s derived from honey shows a strong fluorescence emission centered at 430 nm, which was efficiently quenched by the addition of **MN**. The quenching of fluorescence of **GQDs** by the addition of **MN** (OFF state) and the regaining of quenched fluorescence of **GQDs-MN** system (ON state) upon the addition of the pesticide carbofuran was utilized as a detection strategy for the toxic pesticide carbofuran.

Introduction

The ever increasing demand for food products to meet the world population growth is a challenging concern, which has led to a widespread utilization of pesticides and herbicides in agricultural area to control various pests and weeds. They also help to reduce the loss of crops by decreasing the growth of weeds and eradicating pests.[1] However, the consistent and large use of pesticides not only affect the eco system but also pose detrimental issues on mankind.[2] This includes several metabolic disorders and problems to reproductive and immune system.[3] The US Environmental Protection Agency (USEPA) has classified pesticides into various groups which include organophosphates, pyrethroids, organochlorines, and carbamates.[4] Among the different pesticides available, carbamates are one type of pesticides whose mode of action is similar to that of organo phosphates.[5] Carbofuran (marketed under the trade name *Furadan)*- a carbamate pesticide, has been classified as a harmful substance whose uptake results in severe abnormalities including blurring of vision, breathing difficulty, hyper tension and contact burns to the skin or eyes and fatalities in humans.[6] The ubiquitous usage, high mobility in soil and environmental persistence, results in the contamination of groundwater systems and water bodies.[7] The excessive application of carbofuran has resulted in serious environmental issues of which wildlife poisoning is a major concern.[8] A worldwide ban is enacted and a time bound monitoring of these pesticides is crucial in the present scenario.

Diverse approaches available for the detection of pesticides, include various chromatographic,[9–10] electroanalytical,[11] spectroscopic,[12] and biological-enzyme-linked immunosorbent[13] techniques.[14] Among the various detection strategies, fluorescence based analytical techniques are emerging as a dynamic tool for the detection of pesticides owing to its high sensitivity, simplicity, rapidness, specificity and accessibility.[15–16] Herein, we have developed a fluorescence Turn-On molecular switch derived from naturally occurring α-mangostin (**MN**), isolated from the pericarp of mangosteen fruit and Graphene Quantum Dots (**GQDs**) synthesized from honey for the detection of a toxic pesticide. Development of a sustainable method which is based on the usage of waste material is advantageous instead of using a more severe environmentally hazard synthetic material for the detection of hazardous carbofuran.

Mangosteen (*Garcinia mangostana Linn*) is a tropical tree mainly found in countries like India, Myanmar, Malaysia, Philippines, Sri Lanka, and Thailand, and the fruit is commonly known as queen of fruits. The pericarp of mangosteen fruit contains a variety of secondary metabolites such as prenylated and oxygenated xanthones.[17] Among various xanthone derivatives, α-mangostin (**MN**) is the major one possessing a wide range of biological properties.[18] Even though several reports are available on the biological (pharmacological) applications of **MN**, its optoelectronic properties are less explored. In this paper, we have exploited the fluorescence quenching interaction of **GQDs** with **MN** as a tool for the detection of carbofuran.

GQDs have emerged as promising optical nanomaterials for sensing applications due to their excellent thermal, chemical and photo-stability, biocompatibility and low toxicity.[19] Several methods have been reported to synthesize **GQDs**, which fall

[a] *C. L. Lekshmi, U. S. Swathy, K. Vijayan, H. Simimole, S. Sumalekshmy*
Post Graduate and Research Department of Chemistry
T. K. M. College of Arts and Science
Karicode, Kollam, Kerala, India - 691005
E-mail: suma@tkmcas.ac.in

Supporting information for this article is available on the WWW under https://doi.org/10.1002/slct.202204869

under two main categories namely, top-down and bottom-up approaches. The top-down method involves the cutting of carbonaceous materials into nano-dimensional structures through physical or chemical processes such as oxidation, treatment with acids, electrochemical methods etc. The bottom-up method deals with the synthesis of **GQDs** from components largely of organic origin through processes like carbonization. In the present work, we have used honey as a sustainable and renewable source- for the synthesis of **GQDs** following an emulsion-templated carbonization route.[20] From TEM analysis the average diameter of the synthesised **GQDs** was around 2.4 nm. The lattice parameter of 0.31 nm, the d spacing between graphene layers, corresponds well with that of basal plane distance of bulk graphite i.e. 0.335 nm. (Figure S1, ESI†). **GQDs** display high surface area and the benzene moieties makes them an excellent candidate to be complexed with several compounds. The change in fluorescence properties of a binary system derived by the combination of **GQDs** and **MN** is explored for the selective detection of the harmful pesticide-carbofuran.

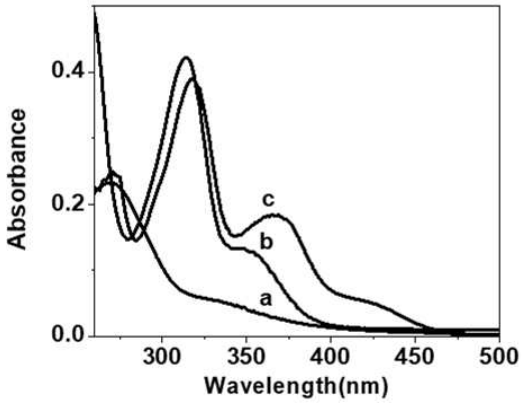

Figure 1. UV-visible spectra of a) **GQDs** (1 mg/mL); b) **MN** (4 μM) and c) **GQD-MN** complex in methanol.

Results and Discussion

The **MN** isolated from the pericarp of mangosteen fruit is found to be analytically pure as shown by HRMS, and NMR analysis. The ^{1}H NMR, ^{13}C NMR, FTIR and HRMS, spectra are shown in Figure S2–S5, ESI†

The absorption spectra of **GQDs**, **MN** and **GQDs-MN** complex in methanol are shown in Figure 1. The spectrum of **GQDs** (Figure 1a) is characterized by a strong absorption peak at 267 nm with a shoulder peak at 340 nm. The absorption peak at 267 nm is due to π-π* transition of C=C and the absorption at 340 nm corresponds to n-π* transition of the C=O bond which is a characteristic feature of **GQDs**. The absorption spectrum of **MN** (Figure 1b) shows a sharp peak at 312 nm with a broad shoulder peak at 353 nm, which may be attributed to n-π* absorption of the carbonyl group. Up on the addition of **GQDs** to **MN**, the UV spectrum showed remarkable changes indicating a ground state interaction between **GQDs** and **MN** (Figure 1c). A shift was observed for **MN** from 353 to 362 nm and 312 to 330 nm and a shift from 267 to 271 nm was observed for **GQDs**.

Upon excitation at 340 nm, **GQDs** exhibited a broad emission band with a maximum at 435 nm (Figure 2-i) and a green luminescence under UV light (inset, Figure 2-i) with a quantum yield of 3.6% (Figure S6, ESI†). **MN** displayed an absorption spectrum in the range of 300 nm to 400 nm where as a solution of **MN** in methanol is non-emissive (Figure 2-ii). Upon adding different concentrations (0 to 4 μM) of **MN** in methanol to the **GQDs** solution, there is a quenching in the intensity of the emission of **GQDs** without any shift in its emission wavelength (Figure 3-i). However, there is no overlap between the emission spectrum of the **GQDs** and the absorption spectrum of **MN**, eliminating the possibility of

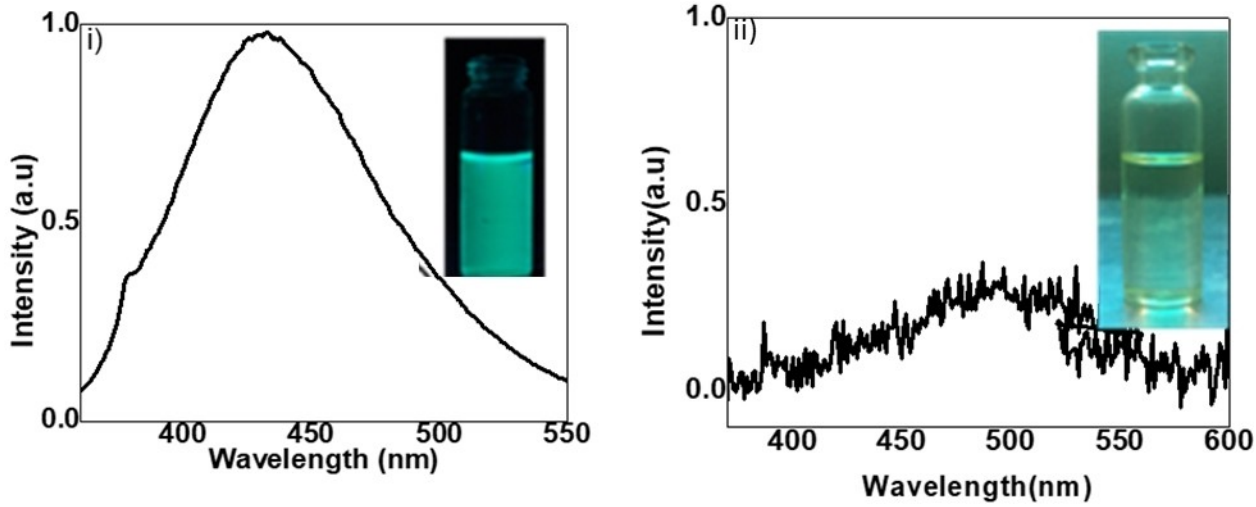

Figure 2. i) Emission spectra of **GQDs**(1 mg/mL) in methanol and inset shows the image of **GQDs** solution in methanol under UV light; ii) Emission spectra of **MN** (1 μM) in methanol and inset shows the image of its methanol solution observed under UV light.

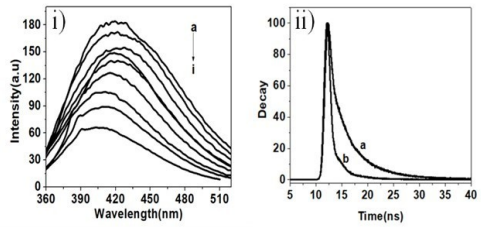

Figure 3. i) Quenching of **GQDs**(1 mg/mL) emission in methanol by addition of **MN** a) 0 μM b) 0.5 μM c) 1 μM d) 1.5 μM e) 2 μM f) 2.5 μM g) 3 μM h) 3.5 μM and i) 4 μM and ii) Decay profile of **GQDs** (a) and **GQDs-MN** complex(b).

fluorescence quenching by fluorescence resonance energy transfer (**FRET**) (Figure S7, ESI†). Hence the possible mechanisms of quenching may be electron transfer assisted by static interactions through hydrogen bonding or π-π interactions between **GQDs** and **MN**. **GQDs** are acting as good electron acceptor[21] and **MN** acts as electron donor. The existence of enolic O,O ligand, methoxy and hydroxyl groups are mainly responsible for the electron donating property of **MN**.[22] Similarly the rigid xanthone moiety in **MN** can involve in π-π stacking interactions with **GQDs**.[23] The surface of **GQDs** possess large number of hydroxyl functional groups, which allow strong hydrogen bonding interaction with **MN** there by contributing to the quenching of fluorescence intensity. The structures of **GQDs** and of **MN** are represented in Figure S8, ESI†.

The excited state quenching mechanism of **GQDs** was investigated via fluorescence lifetime (τ) measurements. The fluorescence lifetimes of **GQDs** and **GQD-MN** were analyzed using time resolved photoluminescence measurements using 340 nm LED source (Figure 3-ii). The decay curve is best fitted with multi exponential function which indicates the presence of multiple radiative species in the samples. Hence, it is preferable to consider the average lifetimes of the decaying species present in the molecules.[24] The average lifetime of the **GQDs** and **GQDs-MN** are found to be 6.2 and 3.8 ns respectively. The decrease in the average lifetime of **GQDs-MN** demonstrates that the quenching may be dynamic in nature indicating the involvement of PET with in the complex.[25]

The fluorescence quenching behavior was then analyzed using Stern–Volmer (S–V) relation[26–27] [1],

$$I_0/I = 1 + K_{SV}[Q] \quad (1)$$

where, I_0 is the fluorescence intensity of **GQDs** solution without adding **MN**, I is that after adding **MN**, K_{SV} is Stern Volmer constant and [Q] is the final concentration of **MN**. Figure S9, ESI represents the S–V plot and a good linearity is observed with a correlation coefficient of 0.99 for the initial concentrations and a slight deviation at higher concentration. This linear Stern–Volmer plot indicates the involvement of a dynamic quenching phenomenon.[28] For **GQD-MN** system even though there is a possibility for the occurrence of quenching through dynamic mode, a slight deviation in the S–V plot shows the possibility of static quenching.[29] The K_{SV} value of $2.78\times10^4\ M^{-1}$ clearly indicates high quenching efficiency of fluorescence of **GQDs** by **MN**.

We have exploited the fluorescence behaviour of **GQDs** in the presence of **MN** to develop a platform for the detection of the pesticide carbofuran. For this, varying concentrations of carbofuran was added to a mixture of **GQDs** and **MN**. A regular enhancement in fluorescent intensity was observed, which is due to the spontaneous release of **MN** from the complex, represented in Figure 4-i. Figure 4-ii shows the calibration curve which is the the plot of fluorescence enhancement efficiency (FEE) at the maximum emission peak (430 nm) against the concentration of carbofuran. The plot is linear within a range from 2 to 5 μM where the calibration equation [2] is used.

$$FEE_{carbofuran} = 0.2577\ C_{carbofuran} + 0.523 \quad (2)$$

The enhancement in fluorescence intensity is also evident from the time resolved fluorescent analysis. When carbofuran was added to the complex, the average life time was changed from 3.8 to 5.92 ns. (Fig S10, ESI†.) This enhancement in the lifetime is due to the dissociation of **GQDs-MN** complex, releasing the **MN** to the solution owing to the higher binding affinity of carbofuran to **GQDs**.

The interactions of carbofuran with **GQDs** and the release of **MN** in the **GQDs-MN** complex were confirmed by conducting control experiments. For this different concentrations of carbofuran were added to **GQDs** solution. The fluorescence intensity of GQDs was more or less unaffected by the presence of carbofuran (Figure S12, ESI†). Also the absorption spectra of MN didn't show much change up on the addition of carbofuran ruling out the possibility of any ground state interaction between these two compounds (Fig S11, ESI†). Therefore, it is proposed that the interaction of carbofuran with **GQDs-MN** complex releases **MN** from the complex and regains the fluorescence of **GQDs** (Scheme 1).

The stoichiometry for interaction of carbofuran with **GQDs-MN** complex and the association constant was determined by using the Benesi-Hildebrand analysis. In the presence of carbofuran, 1:1 stoichiometry (which is confirmed from the straight line graph) is observed for the complex with an association constant (K_{ass}) of $4.33\ M^{-1}$. (Figure S13 b, $R^2 = 0.99389$, ESI†). In a similar manner the binding constant for the

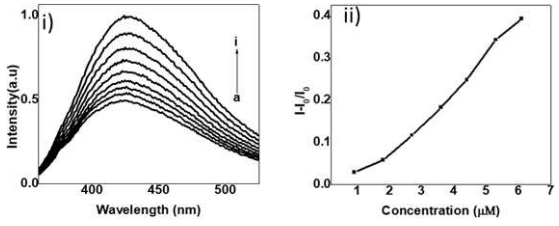

Figure 4. i) Fluorescence spectra of **GQDs-MN** (1 mg/mL) with different concentration ranging from a) 0 to i) 7 μM of carbofuran in methanol ii) Calibration plot.

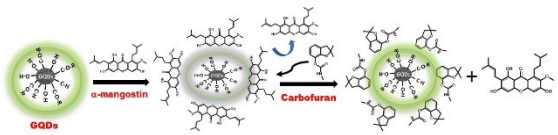

Scheme 1. Pictorial representation of the detection process

interaction of **MN** with **GQDs** was obtained as 1.0235 M^{-1} (Figure S13 a). The detection limit was found to be 0.01 μM (Fig S14, ESI†). The selectivity of the **GQDs-MN** system is investigated by comparing the effect of fluorescence intensity of different pesticides other than carbofuran on the **GQDs-MN** system. It has been noted that among the various pesticides used-carbaryl (Cl), parathion (PT), thiabendazole (TBZ), cypermethrine (CM), and malathion (MT), the **GQDs-MN** system has high degree of selectivity for carbofuran. (Figure S15, ESI†).

Conclusion

The fluorescence changes of **GQDs** in the presence of **MN** and carbofuran is exploited to develop a fluorescent sensor for the toxic pesticide carbofuran with a detection limit of 0.01 μM. The fluorescence emission of **GQDs** was efficiently quenched by **MN**, which regained up on the addition of carbofuran there by acting as a Turn-On molecular switch for the detection of this pesticide.

Experimental Section

Isolation of α-Mangostin (MN): MN was isolated following a reported procedure[17,30] which was later modified to improve the yield by subjecting the powdered pericarp to Soxhlet extraction using ethyl acetate as the solvent. This extract was collected, the solvent removed under reduced pressure and the residue was purified by column chromatography on silica gel (60–120 mesh) with the n-hexane-ethyl acetate as the solvent system to get analytically pure **MN** as an yellow crystalline solid in 69% yield with respect to the crude residue.

Synthesis of Graphene Quantum Dots (GQDs): The **GQDs** were synthesized following a previously reported literature procedure.[20] In this method, aqueous solutions of honey are emulsified in 1-butanol in which the hydroxyl functional group could stabilize the emulsions against coalescence. Since each emulsion contains a limited amount of honey molecule, the formation of undesirable bulk structures would be prevented. This will act as micro reactors. The nearly monodispersed **GQDs** were synthesized via carbonization of honey molecules allocated in water-in-oil emulsions. To form the emulsions, a 10 wt% honey solution (aq.) was mixed with 1-butanol and the mixture was aged at 80 °C under vigorous stirring for 1 h. To the mixture a catalytic amount of hexadecylamine was then added and the temperature was elevated to 160 °C under argon to initiate the carbonization. The as-prepared **GQDs** were purified by centrifuging and finally dissolved in methanol.

Acknowledgements

The authors are grateful to Professor Kuruvilla Joseph, Registrar and Dean, IIST, Trivandrum for his helpful comments and valuable discussions. We extent our sincere gratitude to Dr. Joshy Joseph, Principal Scientist, CSIR-NIIST, Trivandrum for his guidance throughout the work. We also thank financial assistance from DST-SERB (SB/FT/CS-116/2012 dated 08.07.2014), DST-FIST and CSIR.

Conflict of Interest

The authors declare no conflict of interest.

Data Availability Statement

The data that support the findings of this study are available in the supplementary material of this article.

Keywords: α-mangostin · Graphene Quantum Dots · Fluorescence Quenching · photophysics · Pesticides

[1] N. Kazemifard, A. A. Ensafi, B. Rezaei, *Food Chem.* **2020**, *310*, 125812.
[2] V. Bind, A. Kumar, *MOJ Toxicol.* **2019**, *5*, 17–18.
[3] R. Umapathi, B. Park, S. Sonwal, G. M. Rani, Y. Cho, Y. S. Huh, *Trends Food Sci. Technol.* **2022**, *119*, 69–89.
[4] O. Bashir, S. A. Bhat, A. Basharat, M. Qamar, S. A. Qamar, M. Bilal, H. M. Iqbal, *Chemosphere* **2022**, *292*, 133320.
[5] J. A. Vale, S. M. Bradberry, *Critical Care Toxicology: Diagnosis and Management of the Critically Poisoned Patient* (Eds.: J. Brent, K. Burkhart, P. Dargan, B. Hatten, B. Megarbane, R. Palmer, J. White), Springer International Publishing, Cham, **2017**, pp. 1829–1853.
[6] P. O. Otieno, J. O. Lalah, M. Virani, I. O. Jondiko, K.-W. Schramm, *J. Environ. Sci. Health Part B* **2010**, *45*, 137–144.
[7] M. Syafrudin, R. A. Kristanti, A. Yuniarto, T. Hadibarata, J. Rhee, W. A. Al-onazi, T. S. Algarni, A. H. Almarri, A. M. Al-Mohaimeed, *Int. J. Environ. Res. Public Health* **2021**, *18*, 468.
[8] S. Radhakrishnan, *Eur. J. Wildl. Res.* **2018**, *64*, 58.
[9] L. E. Vera-Avila, B. P. Márquez-Lira, M. Villanueva, R. Covarrubias, G. Zelada, V. Thibert, *Talanta* **2012**, *88*, 553–560.
[10] J. Borrull, A. Colom, J. Fabregas, E. Pocurull, F. Borrull, *Anal. Bioanal. Chem.* **2019**, *411*, 1601–1610.
[11] D. Gonçalves-Filho, C. C. G. Silva, D. De Souza, *Talanta* **2020**, *212*, 120756.
[12] F. Donato, M. Kemmerich, J. F. Facco, C. A. Friggi, O. Prestes, M. Adaime, R. Zanella, *Braz. J. Anal. Chem.* **2012**, *2*, 331–340.
[13] D. Sahoo, A. Mandal, T. Mitra, K. Chakraborty, M. Bardhan, A. K. Dasgupta, *J. Agric. Food Chem.* **2018**, *66*, 414–423.
[14] I. Kaur, V. Batra, N. Kumar Reddy Bogireddy, S. D. Torres Landa, V. Agarwal, *Food Chem.* **2023**, *406*, 135029.
[15] N. I. M. Fauzi, Y. W. Fen, N. A. S. Omar, H. S. Hashim, *Sensors* **2021**, *21*, 3856.
[16] X. Zhang, X. Liao, Y. Hou, B. Jia, L. Fu, M. Jia, L. Zhou, J. Lu, W. Kong, *J. Hazard. Mater.* **2022**, *422*, 126881.
[17] W. Schmid, *Justus Liebigs Ann. Chem.* **1855**, *93*, 83–88.
[18] T. Chavan, A. Muth, *Future Med. Chem.* **2021**, *13*, 1679–1694.
[19] T. Ghosh, S. Chatterjee, E. Prasad, *J. Phys. Chem. A* **2015**, *119*, 11783–11790.
[20] S. Mahesh, C. L. Lekshmi, K. D. Renuka, K. Joseph, *Part. Part. Syst. Charact.* **2016**, *33*, 70–74.
[21] M. Suryaman, Y. Sunarya, I. Istarimila, A. Fudholi, *Biocatal. Agric. Biotechnol.* **2021**, *36*, 102132.
[22] Y. Liu, L. Ma, W.-H. Chen, H. Park, Z. Ke, B. Wang, *J. Phys. Chem. B* **2013**, *117*, 13464–13471.

[23] Y. Y. Ju, X. X. Shi, S. Y. Xu, X. H. Ma, R. J. Wei, H. Hou, C. C. Chu, D. Sun, G. Liu, Y. Z. Tan, *Adv. Sci.* **2022**, 2105034.
[24] N. Dhenadhayalan, C. Selvaraju, *J. Phys. Chem. B* **2012**, *116*, 4908–4920.
[25] J. R. Lakowicz, *Principles of Fluorescence Spectroscopy*, 2 ed., Springer New York, NY, **2006**.
[26] S. Xu, S. Xu, Y. Zhu, W. Xu, P. Zhou, C. Zhou, B. Dong, H. Song, *Nanoscale* **2014**, *6*, 12573–12579.
[27] N. Fahimi-Kashani, A. Rashti, M. R. Hormozi-Nezhad, V. Mahdavi, *Anal. Methods* **2017**, *9*, 716–723.
[28] M. H. Gehlen, *J. Photochem. Photobiol. C* **2020**, *42*, 100338.
[29] E. Ciotta, P. Prosposito, R. Pizzoferrato, *J. Lumin.* **2019**, *206*, 518–522.
[30] M. Parveen, N. U.-D. Khan, B. Achari, P. K. Dutta, *Phytochemistry* **1991**, *30*, 361–362.

Submitted: December 15, 2022
Accepted: March 22, 2023